Temperature-induced adsorption and desorption of phosphate on poly(acrylic acid-co-N-[3-(dimethylamino)propyl]acrylamide) hydrogels in aqueous solutions

Baiyou Liu[a], Huayong Luo[a,*], Hongwei Rong[a,*], Xueyang Zeng[a], Kelin Wu[a], Zuhao Chen[a], Hanxing Lu[a], Dongchuan Xu[b]

[a]*School of Civil Engineering, Guangzhou University, Guangzhou, 510006, China, Tel. +86 20 39366657, Fax +86 20 39366657, email: liubaiyou94@163.com (B. Liu), lhy0909@gzhu.edu.cn (H. Luo), gzdxrhw@163.com (H. Rong), 183362493@qq.com (X. Zeng), 522959062@qq.com (K. Wu), 493947832@qq.com (Z. Chen), 476448531@qq.com (H. Lu),*
[b]*School of Harbin Institute of Technology, Harbin, 150000, China, email: 15161777@qq.com (D. Xu)*

ABSTRACT

We explore the feasibility of using thermosensitive hydrogels based on copolymers of acrylic acid (AAC) and *N*-[3-(dimethylamino)propyl] acrylamide (DMAPAA) [P(AAC-*co*-DMAPAA)] for adsorption and desorption of phosphate in aqueous solutions by a temperature swing. The hydrogels were protonated when they swelled in acidic solution at room temperature, exhibiting good adsorption capacity of phosphate. The phosphate ions were desorbed at high temperature due to the ionic repulsion of carboxyl groups caused by the dissociation of hydrogen bonding. The hydrogels were characterized by Fourier transform infrared spectroscopy (FTIR), scanning electron microscopy (SEM) and thermogravimetric analysis (TGA). The effects of solution pH and temperature on phosphate removal were investigated. Kinetic data revealed that the adsorption of phosphate fitted the pseudo-first-order model. Isotherm data showed that the Freundlich model was more suitable than the Langmuir model. Effective desorption of phosphate was observed by raising the solution temperature to 55°C, and repeated adsorption and desorption behaviors were achieved within three consecutive cycles by a temperature swing between 25°C and 55°C. These findings suggest the possible phosphate removal and recovery from aqueous solutions by changing the environmental temperature.

Keywords: Thermosensitive; Hydrogel; Adsorption; Desorption; Phosphate

1. Introduction

Phosphorus is a limited and non-renewable resource, which is viewed as an essential element both for human development and plant growth [1,2]. However, the eutrophication due to excess phosphorus discharged into water body is a serious problem, which can cause algal blooms and deterioration of water quality. Thus, it is necessary to find a simple and effective method to remove and recycle phosphorus from wastewater [3,4]. At present, various technologies for removing phosphorus from aqueous solutions have been developed, such as membrane filtration [5], ion exchange [6], chemical precipitation [7], biological removal [8], and adsorption [9–11]. Among these methods, adsorption is considered as an attractive alternative due to its simple operation, low cost, steady phosphorus removal, and potential for phosphorus recovery [12]. To date, a variety of adsorbents such as clay mineral [13], industrial byproduct [14], synthetic metal oxide/hydroxide nanomaterials [8,15] and bio-polymer beads [3,9–11] have been explored and applied for the adsorptive removal and recovery of phosphorus from polluted water. However, the aforementioned adsorption methods usually need strong alkaline solutions (NaOH) to desorb phosphate ions from the phosphate-loaded adsorbents for the regeneration. The used alkaline solutions may then become potential second-

*Corresponding author.

ary waste. Therefore, more simple process to remove and recover the phosphorus from aqueous solutions with lower secondary waste production is required.

In recent years, there has been a growing interest in focusing on the development of novel hydrogels and their applications in various fields, including environmental remediation and pollution control [16]. Hydrogels are three-dimensional network polymers, which have strong ability to maintain water and adsorb water-soluble contaminations while keeping their shape [17]. Besides, functional hydrogels can exhibit an abrupt change in volume in response to external stimuli such as temperature, pH and ion intensity [18]. For example, thermo sensitive poly(*N*-isopropylacrylamide) (PNIPAM)-based hydrogels can produce an abrupt reversible phase transition in aqueous media, which swell below the volume phase transition temperature (VPTT), and shrink as the temperature increases [19]. The volume phase transitions of these hydrogels in water are driven by hydrophobic interactions between the macromolecules [20]. Based on this property, thermosensitive hydrogels have been widely used in various fields, including adsorption/desorption of pollutants, regenerative medicine and in situ drug release [18]. Recently, Gotoh's group [21] developed a novel thermosensitive gel adsorbent made by the copolymerization of *N*-isopropylacrylamide (NIPAM) and *N*-[3-(dimethylamino)propyl]acrylamide (DMAPAA) for phosphate capture. The phosphate ions were adsorbed onto the ionized tertiary amino groups in the gel network below the VPTT and were desorbed above the VPTT due to the ionization suppression of the tertiary amino groups and the shrinkage of the gel [21]. However, the hydrogel exhibited relative low adsorption capacity for phosphate ions, which might be due to that the secondary component (DMAPAA) for capturing phosphate ions was introduced in a very limited amount as compared to primary component of NIPAM, in order to maintain the gelation and thermo sensitivity of copolymeric hydrogels [22].

On the other hand, another kind of thermosensitive hydrogels has been reported that their volume phase transitions are driven by another type of interactions between the macromolecules, i.e. by hydrogen bonding [20,23–26]. Xiao et al. report the synthesis and characterization of mono dispersed thermoresponsive hydrogel microspheres with a volume phase transition driven by hydrogen bonding [20]. The copolymers of *N*,*N*-dimethylaminoethyl methacrylate (DMAEMA) and acrylamide (AM) were prepared to demonstrate a temperature-induced phase transition due to the formation of hydrogen bonds [24]. Kubota et al. showed that the poly(acrylic acid-*co*-acrylamide)-*graft*-oligo(ethylene glycol) hydrogels were temperature-responsive gels that contract at lower temperature and swell at higher temperature [23]. Kim et al. [25] reported that the smart hydrogels composed of poly(acrylic acid) (PAAC)/poly(vinyl sulfonic acid) (PVSA) showed the temperature-dependent behavior, due to the association/dissociation of the hydrogen bonding of the carboxyl groups in the PAAC and the sulfonate groups in the PVSA of the hydrogels. Okano et al. showed that both polyacrylamide (PAM)/poly(acrylic acid) (PAAC) and poly(*N*-acryloylglycinamide) (PAG)/PAAC hydrogels with inter-penetrating polymer networks (IPNs) exhibit collapsed states from formation of inter polymer complexes via hydrogen bonding at lower temperatures

and swollen states from dissociation of these complexes at higher temperatures [26]. Nevertheless, to date, there are few reports on exploring this type of thermosensitive hydrogels for the adsorptive removal and recovery of phosphorus from aqueous solutions.

In the present study, chemically cross-linked thermo sensitive hydrogels were synthesized via free radical copolymerization of AAC and DMAPAA, called P(AAC-*co*-DMAPAA) here. The prepared smart polymeric materials can not only adsorb phosphate ions from aqueous solutions but also be able to release the adsorbed phosphate as a response to thermal stimuli. The protonation of the tertiary amino group from DMAPAA contributes the adsorption of phosphate while the ionic repulsion of the carboxyl groups of AAC at high temperatures controls the release of the adsorbed phosphate from the adsorbent. Herein, the physicochemical characterization of the synthesized hydrogels was conducted by Fourier transform infrared spectroscopy (FTIR), scanning electron microscopy (SEM), and thermogravimetric analysis (TGA). Batch experiments were carried out to examine the effects of solution pH and temperature. Adsorption behaviors of P(AAC-*co*-DMAPAA) were studied by fitting different isotherms and kinetics models. Desorption of phosphate from the hydrogels under a temperature stimulus of 55°C was also evaluated. Additionally, three adsorption-desorption cycles by a temperature swing were investigated to evaluate the potential of as-prepared hydrogels for adsorptive removal and recovery of phosphate from aqueous solutions in a controllable way.

2. Materials and methods

2.1. Materials

N-[3-(dimethylamino)propyl]acrylamide (DMAPAA, 99%), acrylic acid (AAC, 99%), ammonium persulfate (APS, 99%) and *N*,*N*′-methylene bisacrylamide (BIS, 98%) were purchased from Aladdin (Shanghai, China). Hydrochloric acid (HCl), sodium hydroxide (NaOH), and potassium phosphate monobasic (KH_2PO_4) were purchased from Shanghai Experiment Reagent Co. (Shanghai, China) without further purification. Deionized (DI) water (18 MΩ cm) used in the experiments was produced using a water-purification system (TST-P, Shijiazhuang, China).

2.2. Preparation of P(AAC-co-DMAPAA) hydrogels

The P(AAC-*co*-DMAPAA) hydrogel based on AAC and comonomer DMAPAA with a molar ratio of 7:3 was synthesized via the free-radical polymerization [27,28]. Firstly, a weighed quantitative monomer AAC and comonomer DMAPAA were dissolved in DI water to form a 16.7 wt% solution. Then, the cross linker BIS and initiator APS were dissolved in the solution, which was then degassed using bubbling nitrogen for 20 min. The molar ration of monomers, cross linker and initiator was fixed at 100:3:1. The obtained solution was then transferred to plastic tubes with an inner diameter of 5 mm, followed by polymerization in the vacuum oven at 60°C for 24 h. After cross linking, the prepared hydrogels were removed and cut into pieces with

2.0-mm thickness. The hydrogel pieces were then repeatedly washed with DI water every 12 h for 5 d to remove unreacted materials. Finally, the hydrogels were dried under vacuum at 60°C for 24 h and stored for further use. A simplified scheme for the formation of the P(AAC-*co*-DMAPAA) hydrogel is given in Fig. 1.

2.3. Material characterization

The morphology of P(AAC-*co*-DMAPAA) hydrogels was characterized by SEM (Sigma 300, Germany). The functional groups of hydrogels were analyzed by FTIR spectroscopy (Tensor 27, Bruker, Germany). The thermogravimetric analysis (TGA) and differential thermogravimetry (DTG) were carried out by thermogravimetric analyzer (TA-60Ws, Japan) in nitrogen atmosphere under a heating rate of 10°C/min varying from room temperature to 800°C. The point of zero charge (pH_{pzc}) for the hydrogels was determined by the pH shift method [9,11,29]. The initial pH (pH_i) and final pH (pH_f) were determined by a pH electrode (PB-10, Sartorius, Germany). The value of pH_{PZC} is the point at which the curve of $\Delta pH = (pH_i – pH_f)$ versus pH_i crosses the line equal to zero. When the solution pH is lower than pH_{PZC}, the surface of the adsorbent is positively charged, while the surface of the adsorbent is negatively charged when the solution pH is higher than pH_{PZC} [30].

2.4. Batch studies

The batch adsorption experiments were performed by adding 0.05 g dry hydrogel to a 50-mL tube containing 20-mL phosphate solution with a desired pH (initial phosphate concentration = 150 mg/L). KH_2PO_4 was used to prepare the phosphate solution with the concentration based on phosphorus only. The phosphate concentration was determined by the ammonium molybdate spectrophotometric method [11]. The tubes were placed in a temperature-controlled shaker (THZ-82A, Kexing, China) to vibrate at 140 rpm for 24 h. The adsorption capacity of the hydrogel was evaluated using Eq. (1).

$$q_t = \frac{(C_o - C_t) \times V}{m} \tag{1}$$

where q_t (mg/g) is the adsorption capacity of the hydrogel at t (h) time; C_0 and C_t (mg/L) represent the phosphate concentration before and after adsorption, respectively; V (L) is the volume of the original solution, and m (g) is the mass of dry hydrogel.
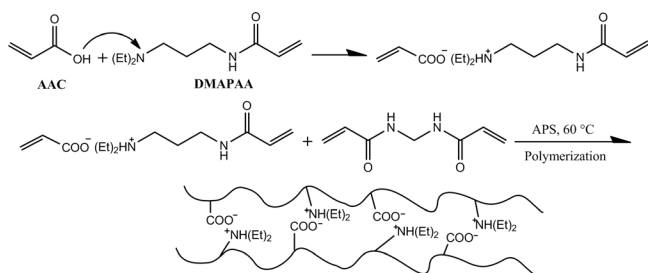
The effect of pH on phosphate adsorption was determined over a range of initial pH values from 2.0 to 10.0 at 25°C, which were adjusted by 0.1 mol/L HCl and 0.1 mol/L NaOH solutions. The effect of temperature was evaluated by varying temperature in the range of 25–55°C at pH 2.0. The adsorption kinetics was conducted at an initial phosphate concentration of 150 mg/L, pH 2.0 and 25°C. Samples were collected at predetermined time intervals for concentration analysis. The adsorption isotherms were evaluated at pH 2.0 with an initial phosphate concentration varying from 25 to 150 mg/L, at 25°C for 24 h to reach equilibrium.

After adsorption equilibrium at 25°C, the temperature of the original solution was increased to 55°C for desorption of phosphate ions, and their concentration was measured. The desorption ratio is determined as the ratio of the desorbed phosphate amount to that adsorbed.

2.5. Data modeling

Langmuir and Freundlich isotherm models were used to decipher the adsorption equilibrium. Langmuir [Eq. (2)] and Freundlich [Eq. (3)] isotherms can be expressed as follows [9,11,29].

$$q_e = \frac{q_{max} k_L C_e}{1 + k_L C_e} \tag{2}$$

$$q_e = k_F C_e^{1/n} \tag{3}$$

where q_e (mg/g) and C_e (mg/L) represent the adsorption capacity of adsorbents at equilibrium from experiment and the equilibrium concentration of phosphate, respectively; k_L (L/mg) and q_{max} (mg/g) are the Langmuir constant and the predicted maximum adsorption capacity, respectively; k_F (mg/g) and n denote the Freundlich constant and the heterogeneity factor, respectively.

The pseudo-first-order model and pseudo-second-order model were applied to identify the key process controlling the adsorption rate. The pseudo-first-order [Eq. (4)] and pseudo-second-order [Eq. (5)] kinetic models are given as follows [29].

$$q_t = q_e(1 - e^{-k_1 t}) \tag{4}$$

$$q_t = \frac{k_2 q_e^2 t}{1 + k_2 q_e t} \tag{5}$$

where q_t and q_e (mg/g) are the adsorption capacities at time t (h) and at equilibrium. k_1 (1/min) and k_2 (g/mg/min) are the rate constants for the pseudo-first-order model and pseudo-second-order model, respectively.

3. Results and discussion

3.1. Characterization

Fig. 2 shows the interior morphology of freeze-dried P(AAC-*co*-DMAPAA) hydrogels. From the SEM micrograph, we can see that the hydrogel had an obvious
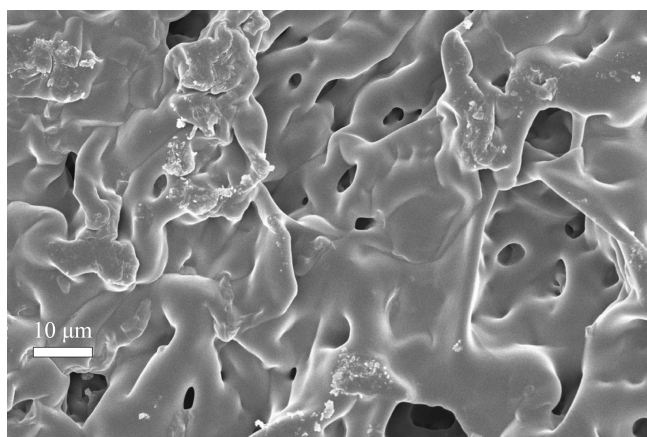

Fig. 1. Schematic preparation of P(AAC-co-DMAPAA) hydrogel.

Fig. 2. SEM image of P(AAC-co-DMAPAA) hydrogel.

Fig. 4. TGA/DTG thermograms of P(AAC-*co*-DMAPAA) hydrogel.

three-dimensional network structure with different pore sizes, which would facilitate the adsorbate molecules to diffuse into the adsorbent and access adsorptive sites [9].

Fig. 3 shows the FTIR spectra of P(AAC-*co*-DMAPAA) hydrogels. The characteristic peak located at 1716 cm^{-1} is due to the stretching vibration of carboxyl carbonyl group (C=O of COOH) which results from AAC monomer [31,32]. The strong peaks at 1646 cm^{-1} and 1559 cm^{-1} can be ascribed to the stretching vibration of amide I and amide II peaks that result from DMAPAA monomer [33]. Besides, the peak at 2950 cm^{-1} corresponds to the combined stretching of CH$_2$ groups in both the AAC and DMAPAA monomers, while the broad absorption bands in the 3100 to 3500 cm^{-1} region are due to the overlapping absorption bands of O-H and N-H stretching [34]. These results certainly confirm the copolymerization of AAC with DMAPAA.

Fig. 4 shows the TGA/DTG thermograms of P(AAC-*co*-DMAPAA) hydrogels in the range of 25°C–800°C. The first weight loss of 19.7% in the range of 25°C–192°C could be due to the evaporation of trapped and physisorbed water molecules from samples [9]. The weight loss of 21.6% was
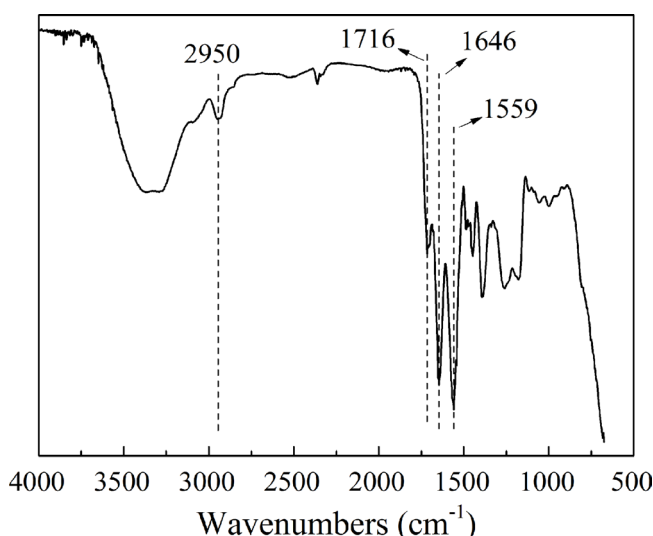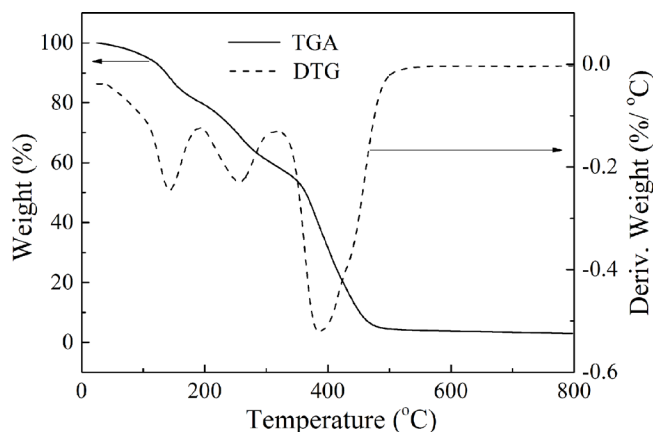
observed by heating from 192°C–317°C, which might be attributed to the thermal decomposition of functional groups such as –OH on the backbone of the hydrogels [35]. The hydrogel weight decreased gradually when the temperature exceeded 317°C, which was mainly assigned to the further the thermal degradation of the backbone chain [34]. These results indicated that the P(AAC-*co*-DMAPAA) hydrogel was thermally stable when the operating temperature was less than 192°C.

3.2. Batch studies

3.2.1. Effect of pH

The solution pH is an important factor in the adsorption process as it often affects the active sites of the adsorbent surface. The effect of pH on the adsorption of phosphate onto the P(AAC-*co*-DMAPAA) hydrogels was examined with a range of pH from 2.0 to 10.0 at 25°C (Fig. 5). It was found that the adsorption of phosphate was highly dependent on the solution pH. The phosphate adsorption capacity rapidly decreased when the solution pH increased from 2.0 to 10.0. This can be explained as that the surface of
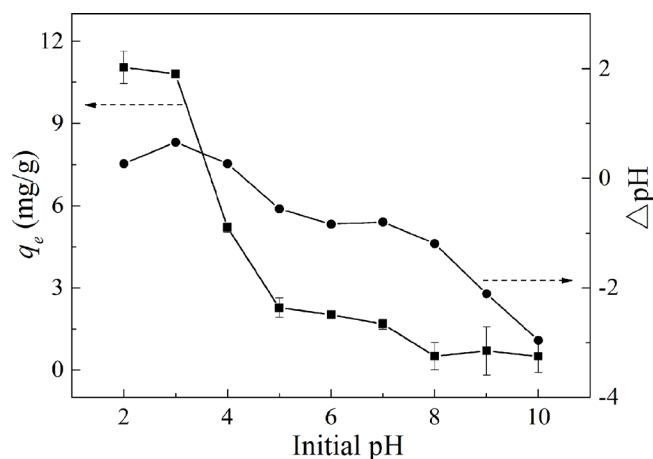

Fig. 3. FTIR spectra of P(AAC-co-DMAPAA) hydrogel.

Fig. 5. Effect of solution pH on phosphate adsorption.

P(AAC-*co*-DMAPAA) hydrogel aggregates more negatively charged because of existing OH⁻ ions at high pH values, resulting in a strong competition between the phosphate and OH⁻ ions for surface active sites of the adsorbent. Similar results have also been observed by other phosphate adsorbents in previous studies [10,36]. Besides, the pH_{pzc} of P(AAC-*co*-DMAPAA) hydrogel was found to be around 4.0, which is indicative of protonation of surface charge and transformation to more positively charged surface at pH 2.0 [29]. Therefore, strong electrostatic attraction between negative phosphate ions and positive adsorbent surface would be essential for a higher adsorption capacity. On the other hand, when the solution pH is above pH_{pzc}, the adsorbent surface would be more negatively charged due to deprotonation with increasing solution pH, which induces a consequent electrostatic repulsion between adsorbent and adsorbate, resulting in decreasing adsorption performance. Considering the adsorption performances at different pH values, all further batch adsorption experiments were investigated at pH = 2.0.

3.2.2. Effect of temperature

The effect of temperature, varying from 25°C to 55°C, on the adsorption of phosphate is shown in Fig. 6. It can be seen that the amounts of phosphate adsorbed onto the P(AAC-*co*-DMAPAA) hydrogel are largely dependent on temperature. The phosphate adsorption capacity of P(AAC-*co*-DMAPAA) hydrogel was decreased significantly when the operating temperature was increased from 25°C to 55°C. This phenomenon is likely associated with the thermosensitivity of P(AAC-*co*-DMAPAA) hydrogel driven by hydrogen bonding. At higher temperatures, the hydrogen bonding in the hydrogel may be destroyed, generating carboxylate ions which cause ionic repulsion [25]. This will induce strong charge-charge repulsion between adsorbent and adsorbate, leading to a low adsorption capacity of phosphate. It should be noted that this temperature-responsive behavior presents the possibility of controlling the adsorption/desorption processes by a temperature swing.
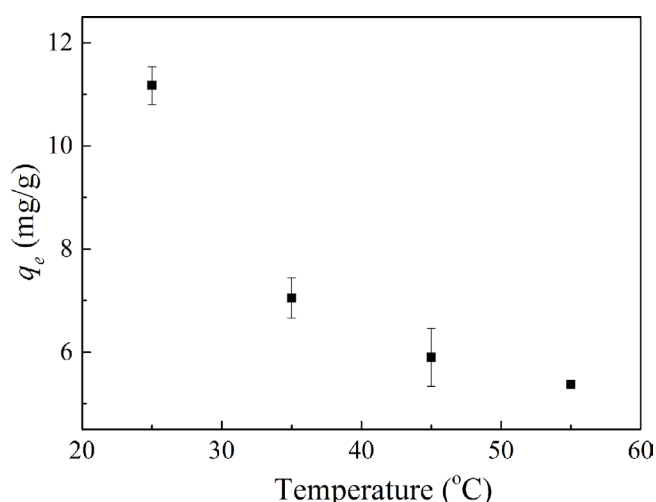
3.2.3. Adsorption isotherms

Fig. 7 shows the adsorption isotherms of phosphate onto P(AAC-*co*-DMAPAA) hydrogels at different initial phosphate levels. It can be seen that the phosphate adsorption capacity by P(AAC-*co*-DMAPAA) increased with the increment of the initial phosphate concentration. This may be due to the increase in the driving force provided by the concentration gradient of phosphate between the aqueous and solid phases [9]. When the initial phosphate concentration was increased to 150 mg/L, the adsorption capacity was found to be 11 mg/g. Compared with the reported thermosensitive NIPAM/DMAPAA gel adsorbent with a uptake capacity of ~7 mg/g at an initial phosphate concentration of 5 mM and 20°C [21], the prepared P(AAC-*co*-DMAPAA) exhibited favorable adsorption behavior. The adsorption isotherms of the P(AAC-*co*-DMAPAA) were fitted by Langmuir and Freundlich isotherm models. Table 1 shows that the Freundlich fitting curve exhibited higher regression constant ($R^2 = 0.998$) than that of Langmuir fitting curve, suggesting that the Freundlich model was more suitable to describe the phosphate adsorption behavior onto the P(AAC-*co*-DMAPAA) hydrogels. Thus, the adsorption was taken place on the heterogeneous surface of the adsorbent, and multilayer phosphate adsorption was possible [9].
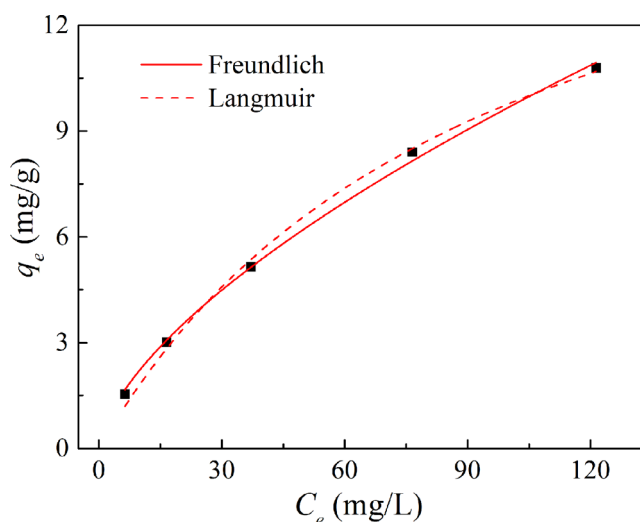

Fig. 7. Fitting adsorption isotherms with Langmuir and Freundlich models at 25°C.

Table 1
The parameters of Langmuir and Freundlich models

Adsorption isotherm	Parameter	Value
Langmuir	k_L (L/mg)	0.011
	q_{max} (mg/g)	19.02
	R^2	0.995
Freundlich	k_F [(mg/g)(L/mg)$^{1/n}$]	0.513
	n	1.567
	R^2	0.998

Fig. 6. Effect of temperature on phosphate adsorption.

3.2.4. Adsorption kinetics

The kinetics of phosphate adsorption by P(AAC-*co*-DMAPAA) is shown in Fig. 8. It was obviously found that the adsorption process of phosphate onto P(AAC-*co*-DMAPAA) was very fast at the initial stage and thereafter the amount of phosphate adsorbed onto the hydrogels increased slowly with increasing contact time until the adsorption equilibrium was reached. The corresponding time to reach the 96.4% of phosphate adsorption capacity was within 5 h. Such a rapid adsorption rate may be a consequence of the electrostatic attraction force between phosphate and P(AAC-*co*-DMAPAA) with more positively charged surface at pH 2.0 [37]. In order to examine the adsorption process, the pseudo-first-order and pseudo-second-order models in Table 2 were used to fit the curves in Fig. 8. The pseudo-first-order model assumes that physisorption limits the adsorption rate of the particles onto the adsorbent, while the pseudo-second-order model considers chemisorption as the rate-limiting mechanism of the process [38]. The obtained kinetic parameters in Table 2 show that the kinetic data was better fitted with pseudo-first-order model than with pseudo-second-order model as reflected by the higher regression constant (R^2). The predicted maximum adsorption capacity of pseudo-first-order model was close to the experimental data (10.8 vs. 11.0) at an initial phosphate concentration of 150 mg/L. This phenomenon indicated that the adsorption process can be defined by the pseudo-first-order kinetic model, suggesting that the adsorption rate of phosphate onto the P(AAC-*co*-DMAPAA) hydrogels is controlled by physisorption.
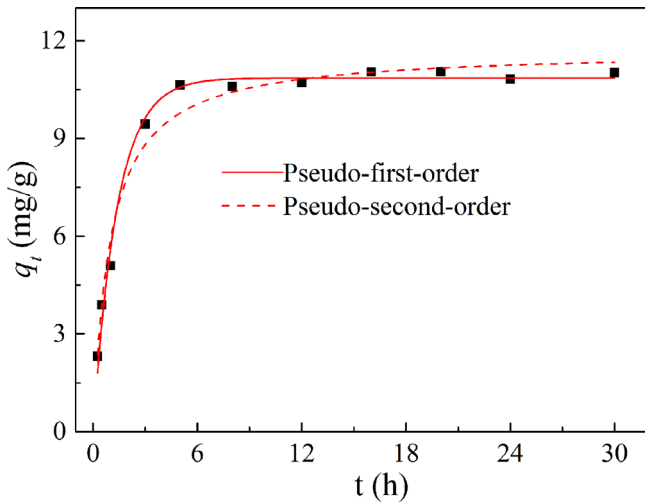
3.2.5. Desorption and re-usability

The phosphate adsorbed onto the P(AAC-*co*-DMAPAA) hydrogels was desorbed by a temperature stimulus (55°C). The results of desorption are shown in Fig. 9. It can be seen that the desorption ratio increased rapidly in the first 3 h and reached equilibrium at approximately 12 h of contact time. Thus, it is easy to achieve the regeneration of P(AAC-*co*-DMAPAA) hydrogels by simply changing the temperature. In order to evaluate the re-usability of the P(AAC-*co*-DMAPAA) hydrogels, the control of adsorption
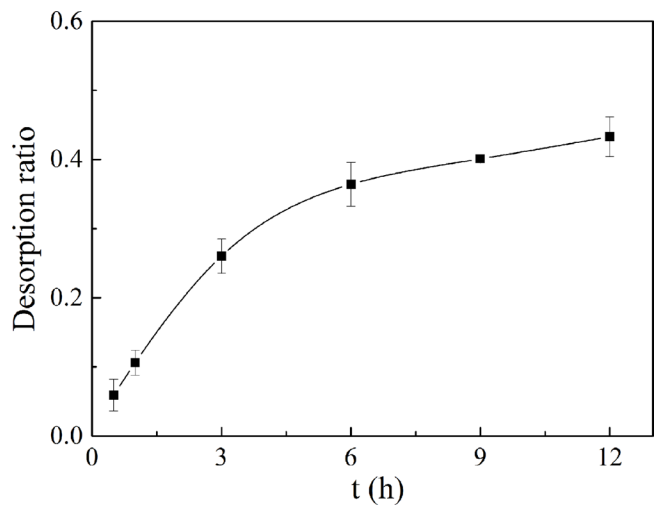

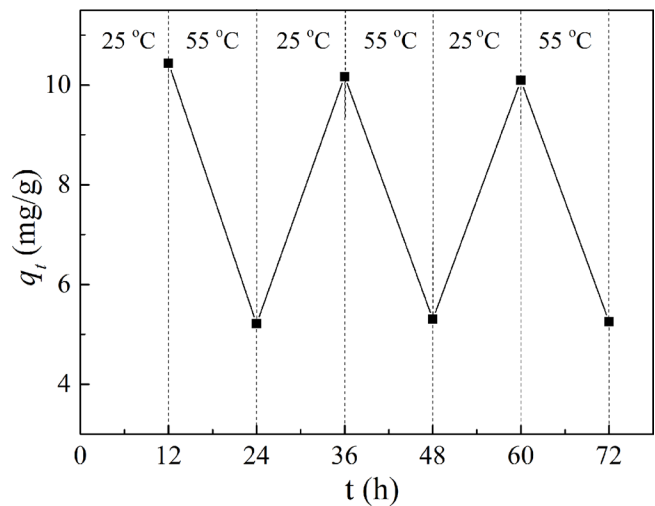Fig. 9. Desorption of phosphate from hydrogels as a function of time at 55°C.

Fig. 8. Pseudo-first-order and pseudo-second-order kinetic model fitting.

Fig. 10. Changes in the amount of phosphate adsorbed to hydrogels by temperature swing.

Table 2
Kinetic model parameters for phosphate adsorption onto P(AAC-co-DMAPAA)

Initial concentration C_o (mg/L)	q_e (mg/g)	Pseudo-first-order			Pseudo-second-order		
		$q_{e(cal)}$ (mg/g)	k_1 (1/min)	R^2	$q_{e(cal)}$ (mg/g)	k_2 (g/mg/min)	R^2
150	11.0	10.8	0.726	0.988	11.7	0.08	0.978

and desorption of phosphate by temperature swing was investigated. The temperature was repeatedly changed between 25°C and 55°C, and the adsorption capacity was measured. The results are illustrated in Fig. 10. The amount of phosphate onto P(AAC-*co*-DMAPAA) is high at 25°C and low at 55°C, that is, the P(AAC-*co*-DMAPAA) hydrogels adsorb and desorb reversibly [39]. The adsorption capacities of the hydrogels repeatedly changed with the temperature swing, and remained stable at each temperature throughout all three cycles. The results indicate the feasibility of the P(AAC-*co*-DMAPAA) hydrogel for phosphate recovery and its repeated use.

4. Conclusions

In this study, we fabricated thermosensitive P(AAC-*co*-DMAPAA) hydrogels via free radical copolymerization for phosphate capture in a controlled way. The optimum adsorption capacity of phosphate was observed at pH 2, and the adsorption capacity decreased with increasing temperatures from 25°C to 55°C. The adsorption of phosphate onto P(AAC-*co*-DMAPAA) could be well fitted to the pseudo-first-order model, and the rate-limiting step was physisorption. The applicability of the Freundlich isotherm model suggested that a multilayer adsorption occurred between the hydrogel adsorbent and phosphate. The recycling of P(AAC-*co*-DMAPAA) hydrogels for phosphate adsorption was possible when the subsequent desorption was carried out at 55°C. Phosphate ions could be repeatedly adsorbed and desorbed by temperature swings between 25°C and 55°C. The as-synthesized P(AAC-*co*-DMAPAA) hydrogels are expected to be a simple, effective and easy-regeneration adsorbent for the removal and recovery of phosphate from aqueous solutions.

References

[1] B.E. Rittmann, B. Mayer, P. Westerhoff, M. Edwards, Capturing the lost phosphorus, Chemosphere, 84 (2011) 846–853.
[2] P. Loganathan, S. Vigneswaran, J. Kandasamy, N.S. Bolan, Removal and recovery of phosphate from water using sorption, Crit. Rev. Environ. Sci. Technol., 44 (2014) 847–907.
[3] J. Wan, C. Zhu, J. Hu, T.C. Zhang, D. Richter-Egger, X. Feng, A. Zhou, T. Tao, Zirconium-loaded magnetic interpenetrating network chitosan/poly(vinyl alcohol) hydrogels for phosphorus recovery from the aquatic environment, Appl. Surf. Sci., 423 (2017) 484–491.
[4] J. Wan, T. Tao, Y. Zhang, X. Liang, A. Zhou, C. Zhu, Phosphate adsorption on novel hydrogel beads with interpenetrating network (IPN) structure in aqueous solutions: kinetics, isotherms and regeneration, RSC Adv., 6 (2016) 23233–23241.
[5] Y. Yang, J. Lohwacharin, S. Takizawa, Hybrid ferrihydrite-MF/UF membrane filtration for the simultaneous removal of dissolved organic matter and phosphate, Water Res., 65 (2014) 177–185.
[6] B. Alyuz, S. Veli, Kinetics and equilibrium studies for the removal of nickel and zinc from aqueous solutions by ion exchange resins, J. Hazard. Mater., 167 (2009) 482–488.
[7] A.H. Caravelli, C. De Gregorio, N.E. Zaritzky, Effect of operating conditions on the chemical phosphorus removal using ferric chloride by evaluating orthophosphate precipitation and sedimentation of formed precipitates in batch and continuous systems, Chem. Eng. J., 209 (2012) 469–477.
[8] Y. Su, H. Cui, Q. Li, S. Gao, J.K. Shang, Strong adsorption of phosphate by amorphous zirconium oxide nanoparticles, Water Res., 47 (2013) 5018–5026.
[9] H. Luo, H. Rong, T.C. Zhang, X. Zeng, J. Wan, Amino–functionalized magnetic zirconium alginate beads for phosphate removal and recovery from aqueous solutions, J. Appl. Polym. Sci., 136 (2019) 46897.
[10] S. Shan, H. Tang, Y. Zhao, W. Wang, F. Cui, Highly porous zirconium-cross linked graphene oxide/alginate aerogel beads for enhanced phosphate removal, Chem. Eng. J., 359 (2019) 779–789.
[11] H. Luo, X. Zeng, P. Liao, H. Rong, T.C. Zhang, Z.J. Zhang, X. Meng, Phosphorus removal and recovery from water with macroporous bead adsorbent constituted of alginate-Zr^{4+} and PNIPAM-interpenetrated networks, Int. J. Biol. Macromol., 126 (2019) 1133–1144.
[12] T.A. Nguyen, H.H. Ngo, W.S. Guo, T.Q. Pham, F.M. Li, T.V. Nguyen, X.T. Bui, Adsorption of phosphate from aqueous solutions and sewage using zirconium loaded okara (ZLO): Fixed-bed column study, Sci. Total. Environ., 523 (2015) 40–49.
[13] J. Chen, L. Yan, H. Yu, S. Li, L. Qin, G. Liu, Y. Li, B. Du, Efficient removal of phosphate by facile prepared magnetic diatomite and illite clay from aqueous solution, Chem. Eng. J., 287 (2016) 162–172.
[14] Z. Zha, Y. Ren, S. Wang, Z. Qian, L. Yang, P. Cheng, Y. Han, M. Wang, Phosphate adsorption onto thermally dehydrated aluminate cement granules, RSC Adv., 8 (2018) 19326–19334.
[15] R. Chitrakar, S. Tezuka, A. Sonoda, K. Sakane, K. Ooi, T. Hirotsu, Selective adsorption of phosphate from seawater and wastewater by amorphous zirconium hydroxide, J. Colloid Interface Sci., 297 (2006) 426–433.
[16] M. Khan, I.M.C. Lo, A holistic review of hydrogel applications in the adsorptive removal of aqueous pollutants: Recent progress, challenges, and perspectives, Water Res., 106 (2016) 259–271.
[17] S. Yu, X. Zhang, G. Tan, L. Tian, D. Liu, Y. Liu, X. Yang, W. Pan, A novel pH-induced thermo sensitive hydrogel composed of carboxymethyl chitosan and poloxamer cross-linked by glutaraldehyde for ophthalmic drug delivery, Carbohydr. Polym., 155 (2017) 208–217.
[18] X. Chen, P. Li, Y. Kang, X. Zeng, Y. Xie, Y. Zhang, Y. Wang, T. Xie, Preparation of temperature-sensitive Xanthan/NIPA hydrogel using citric acid as cross linking agent for bisphenol A adsorption, Carbohydr. Polym., 206 (2019) 94–101.
[19] J. Cheng, G. Shan, P. Pan, Temperature and pH-dependent swelling and copper(ii) adsorption of poly(N-isopropylacrylamide) copolymer hydrogel, RSC Adv., 5 (2015) 62091–62100.
[20] X. Xiao, L. Chu, W. Chen, J. Zhu, Monodispersed thermoresponsive hydrogel microspheres with a volume phase transition driven by hydrogen bonding, Polymer, 46 (2005) 3199–3209.
[21] T. Gotoh, K. Tanaka, T. Arase, S. Sakohara, A novel thermosensitive gel adsorbent for phosphate ions, Macromol. Symp., 295 (2010) 81–87.
[22] Q. Chen, L. Zhu, C. Zhao, J. Zheng, Hydrogels for removal of heavy metals from aqueous solution, J. Environ. Anal. Toxicol., (2012) 2161–0525.

[23] N. Kubota, N. Tatsumoto, T. Sano, Y. Matsukawa, Temperature-responsive properties of poly (acrylic acid-co-acrylamide)-graft-oligo (ethylene glycol) hydrogels, J. Appl. Polym. Sci., 80 (2001) 798–805.

[24] S.H. Cho, M.S. Jhon, S.H. Yuk, H.B. Lee, Temperature-induced phase transition of poly (N, N-dimethylaminoethyl methacrylate-co-acrylamide), J. Polym. Sci. Pol. Phys., 35 (1997) 595–598.

[25] S.J. Kim, S.J. Park, S.I. Kim, Properties of smart hydrogels composed of polyacrylic acid/poly (vinyl sulfonic acid) responsive to external stimuli, Smart Mater. Struct., 13 (2004) 317.

[26] H. Sasase, T. Aoki, H. Katono, K. Sanui, N. Ogata, R. Ohta, T. Kondo, T. Okano, Y. Sakurai, Regulation of temperature-response swelling behavior of interpenetrating polymer networks composed of hydrogen bonding polymers, Makromol. Chem. Rapid Comm., 13 (1992) 577–581.

[27] H. Luo, Q. Wang, T. Tao, T.C. Zhang, A. Zhou, Performance of strong ionic hydrogels based on 2-acrylamido-2-methylpropane sulfonate as draw agents for forward osmosis, J. Environ. Eng., 140 (2014) 04014044.

[28] D. Li, X. Zhang, J. Yao, Y. Zeng, G.P. Simon, H. Wang, Composite polymer hydrogels as draw agents in forward osmosis and solar dewatering, Soft Matter., 7 (2011) 10048–10056.

[29] K.W. Jung, T.U. Jeong, J.W. Choi, K.H. Ahn, S.H. Lee, Adsorption of phosphate from aqueous solution using electrochemically modified biochar calcium-alginate beads: Batch and fixed-bed column performance, Bioresour. Technol., 244 (2017) 23–32.

[30] J. Lin, H. Wang, M. Chu, C. Wang, Y. He, X. Wang, Effect of calcium ion on phosphate adsorption onto hydrous zirconium oxide, Chem. Eng. J., 309 (2017) 118–129.

[31] X. Xiao, R. Zhuo, J. Xu, L. Chen, Effects of reaction temperature and reaction time on positive thermo sensitivity of micro spheres with poly(acrylamide)/poly(acrylic acid) IPN shells, Eur. Polym. J., 42 (2006) 473–478.

[32] A. Das, A.R. Ray, Synthesis and characterization of poly(acrylic acid-co-N-[3-(dimethylamino)propyl]-methacrylamide) hydrogel membranes for biomedical applications, J. Appl. Polym. Sci., 108 (2008) 1273–1280.

[33] S. Saedi, S.S. Madaeni, F. Seidi, A.A. Shamsabadi, S. Laki, Fixed facilitated transport of CO_2 through integrally-skinned asymmetric polyethersulfone membrane using a novel synthesized poly (acrylonitrile-*co*-N,N-dimethylaminopropyl acrylamide), Chem. Eng. J., 236 (2014) 263–273.

[34] N. Limparyoon, N. Seetapan, S. Kiatkamjornwong, Acrylamide/2-acrylamido-2-methylpropane sulfonic acid and associated sodium salt super absorbent copolymer nanocomposites with mica as fire retardants, Polym. Degrad. Stabil., 96 (2011) 1054–1063.

[35] J. Ma, K. Fu, J. Shi, Y. Sun, X. Zhang, L. Ding, Ultraviolet-assisted synthesis of polyacrylamide-grafted chitosan nanoparticles and flocculation performance, Carbohydr. Polym., 151 (2016) 565–575.

[36] X. Luo, X. Wu, Z. Reng, X. Min, X. Xiao, J. Luo, Enhancement of phosphate adsorption on Zirconium hydroxide by ammonium modification, Ind. Eng. Chem. Res., 56 (2017) 9419–9428.

[37] S. Dong, Y. Wang, Characterization and adsorption properties of a lanthanum-loaded magnetic cationic hydrogel composite for fluoride removal, Water Res., 88 (2016) 852–860.

[38] D.A.G. Sumalinog, S.C. Capareda, M.D.G. de Luna, Evaluation of the effectiveness and mechanisms of acetaminophen and methylene blue dye adsorption on activated biochar derived from municipal solid wastes, J. Environ. Manage., 210 (2018) 255–262.

[39] H. Tokuyama, K. Yanagawa, S. Sakohara, Temperature swing adsorption of heavy metals on novel phosphate-type adsorbents using thermo sensitive gels and/or polymers, Sep. Purif. Technol., 50 (2006) 8–14.